

Theoretical Insights into Mooihoekite ($\text{Cu}_9\text{Fe}_9\text{S}_{16}$): A DFT-D Investigation of the bulk properties

K.L Mashishi¹, M.A Mehlape¹, P.P Mkhonto¹ and P.E Ngeope¹

¹Materials Modelling Centre, University of Limpopo, Polokwane, South Africa

E-mail: 201914374@keyaka.ul.ac.za

Abstract. Mooihoekite ($\text{Cu}_9\text{Fe}_9\text{S}_{16}$) is a transition-metal sulfide composed of copper and iron, featuring a metal-rich, tetragonal structure derived from chalcopyrite, and is commonly found as intergrowths with other sulfide minerals in complex ore assemblages. Although it commonly occurs in flotation-relevant ore environments and is known to coexist with minerals such as chalcopyrite and haycockite, its individual flotation behaviour remains poorly explored. This lack of understanding hinders the optimization of separation processes in complex sulfide systems, where phase-specific surface and electronic properties play a critical role. To address this gap, this study employs the dispersion-corrected density functional theory with the incorporation of the Hubbard U parameter to investigate the bulk properties of Mooihoekite. Electronic structure analysis reveals semiconducting behaviour with an approximate band gap of 0.5 eV and antiferromagnetic ordering, depicted by the symmetry in the spin up and down density of states (DOS). Mechanical stability is confirmed through elastic constants that meet the Born criteria, and the calculated Pugh ratio (B/G) indicates ductile behaviour. The computed Debye temperature (318 K) demonstrates reasonable consistency with the experimental data (292 K).

1. Introduction

Transition-metal sulfides represent a geologically significant class of materials distinguished by their structural versatility and functional diversity [1]. These compounds exhibit tunable electronic structures, varied magnetic behaviors, and significant catalytic activity, rendering them essential for a range of applications including energy storage, electrocatalysis, and thermoelectric conversion [2]. Among them, Mooihoekite ($\text{Cu}_9\text{Fe}_9\text{S}_{16}$) stands out as a notable copper-rich iron sulfide, commonly associated with chalcopyrite (CuFeS_2) and pentlandite ($(\text{Fe},\text{Ni})_9\text{S}_8$) within magmatic sulfide assemblages. Mineralogical investigations have shown that Mooihoekite frequently forms intergrowths with haycockite, particularly within hortonolite dunite pegmatites at the Mooihoek Farm locality in Lydenburg, South Africa [3].

Mooihoekite belongs to the chalcopyrite-derived series of sulfides, which are characterized by the incorporation of additional transition-metal atoms into interstitial lattice sites. These modifications give rise to non-stoichiometric compositions that deviate from the ideal CuFeS_2 structure, resulting in altered physicochemical properties. The structure of Mooihoekite is derived from a cubic close-packed arrangement of sulfide anions, with metal cations occupying tetrahedral sites, consistent with a structural lineage related to the Li_2O -type framework. Excess Cu and Fe atoms occupy interstitial voids, contributing to increased metallic content and structural complexity [4]. These modifications are of particular interest in the context of ore processing, as they influence both the thermodynamic stability and reactivity of the mineral under reducing and oxidizing conditions.

Electrochemical investigations have shown that Mooihoekite exhibits moderate oxidative reactivity, performing more efficiently than chalcopyrite but less so than haycockite [5]. This behavior is attributed to its partially open structure, which facilitates electron mobility and the release of constituent metal ions. Thermoelectric studies on nanostructured Mooihoekite synthesized via melting and annealing techniques have revealed semiconducting transport behavior, low lattice thermal conductivity, and tunable electrical properties through Fe doping. A maximum dimensionless figure of merit (zT) of 0.21 at 800 K has been reported for Mooihoekite, highlighting its potential as a functional thermoelectric material. [6]. Magnetic characterization using Mössbauer spectroscopy, magnetic susceptibility, and X-ray diffraction techniques has revealed weak ferromagnetic behavior, with a net magnetic moment of approximately 0.2 μB per formula unit, persisting over a wide temperature range. This response is attributed to partial cation disorder within the tetragonal lattice, in contrast to the higher-symmetry cubic structures observed in related sulfides such as talnakhite. Mössbauer spectra display two distinct hyperfine patterns, indicating that Fe atoms occupy multiple local environments due to structural disorder [7].

Despite the availability of experimental data, comprehensive computational studies of Mooihoekite remain scarce. First-principles methods, particularly the dispersion-corrected density functional theory with Hubbard U corrections (DFT+U), provide a robust framework for investigating the structural, electronic, and mechanical properties of complex sulfides. In this study, dispersion-corrected DFT-D3+U calculations are employed to explore the bulk structural, electronic, and mechanical properties of Mooihoekite.

2. Methodology

The optimized structures of Mooihoekite ($\text{Cu}_2\text{Fe}_9\text{S}_{16}$) were calculated using first-principles density functional theory (DFT) within the Vienna Ab initio Simulation Package (VASP) [8] [9]. Structural optimizations employed the conjugate-gradient algorithm, converging ionic forces to 0.02 eV \AA^{-1} while maintaining self-consistency in the electron density. Valence electron–ionic core interactions were modeled using the projected augmented wave (PAW) method [10] with the electronic exchange–correlation described by the Perdew–Burke–Ernzerhof (PBE) generalized gradient approximation (GGA) functional [11] with the incorporation of the Hubbard U correction (GGA+U) [12]. An effective U_{eff} of 4 eV was able to accurately capture electron correlation in localized Fe d-orbitals, essential for describing Mooihoekite’s structural and electronic properties. Van der Waals interactions were included via the Grimme DFT-D3 method [13] by adding a semi-empirical dispersion function to the conventional Kohn–Sham DFT energy. A plane-wave basis set with a 500 eV kinetic energy cutoff ensured total energy convergence to 10^{-6} eV, with residual Hellman–Feynman forces below 10^{-2} eV \AA^{-1} . The Brillouin zone was sampled with a $4\times 4\times 7$ Monkhorst–Pack k-point mesh [14], while a denser $9\times 9\times 9$ mesh with 0.2 eV width Gaussian smearing was used for electronic structure calculations.

3. Results and discussion

3.1. Bulk structural and thermodynamic properties

Mooihoekite crystallizes in the tetragonal system, with reported lattice parameters of $a = 10.58 \text{ \AA}$ and $c = 5.37 \text{ \AA}$, forming a well-ordered and anisotropic crystal structure (Figure 1). Cu and Fe atoms occupy distinct crystallographic sites within a framework derived from a sphalerite-like arrangement. The structural stability is achieved by additional metal atoms occupying interstitial positions, rather than via cation substitution or sulfur vacancy formation. These interstitial metals exhibit tetrahedral coordination with sulfur atoms ($\sim 2.3 \text{ \AA}$) and octahedral coordination with surrounding metals ($\sim 2.7 \text{ \AA}$), forming Fe–Cu–Fe clusters. DFT-based structural optimization yielded relaxed parameters of $a = 10.458 \text{ \AA}$ and $c = 5.407 \text{ \AA}$, in close-agreement with experimental values (Table 1).

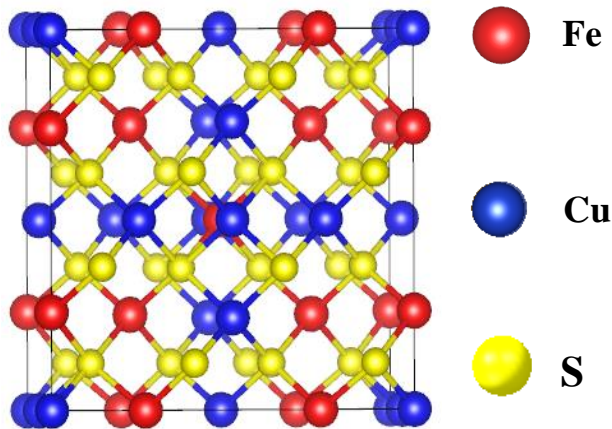


Figure 1. Crystal structure of Moohoekite ($\text{Cu}_9\text{Fe}_9\text{S}_{16}$) with space group p-42m

Structure	Lattice parameters (\AA)	Unit cell volume (\AA^3)	Heats of formation (aV/Atom)
$\text{Cu}_9\text{Fe}_9\text{S}_{16}$	$a=10.45814[10.5800]$ $c=5.40684[5.3700]$	$591.36[603.023]$	-0.76
Interatomic distances (\AA)			
Bonds		Calculated	Experimental
Fe-S		2.279	2.280
Cu-S		2.24	2.330
Fe-Fe		2.749	2.731

Table 1. Structural properties of Moohoekite ($\text{Cu}_9\text{Fe}_9\text{S}_{16}$)

3.2. Mechanical properties

The elastic stiffness tensor relates the stress tensor to the strain tensor through Hooke's law, defining a material's mechanical response. Due to the symmetry of the stress and strain tensors, the elastic stiffness tensor, in its most general form, contains only 21 independent nonzero components [15].

For the tetragonal $\text{Cu}_9\text{Fe}_9\text{S}_{16}$ crystal, the number of independent elastic stiffness components is reduced to five i.e. C_{11} , C_{12} , C_{13} , C_{33} and C_{44} . Here we present the calculated elastic constants, C_{33} , C_{44} , C_{12} and C_{13} , the bulk modulus(B), shear modulus(G), Young's modulus(E), Poisson ratio(ν), and the Pugh ratio in table 3 together with available experimental data.

For a tetragonal crystal, the requirement for mechanical stability leads to the following restrictions on its elastic constants [16]

$$C_{11} > 0, C_{33} > 0, C_{44} > 0, C_{66} > 0; (C_{11} - C_{12}) > 0, (C_{11} + C_{33} - 2C_{13}) > 0; 2(C_{11} + C_{12}) + C_{33} + 4C_{13} > 0$$

The calculated elastic constants of moohoekite satisfy all the mechanical stability criteria for a tetragonal crystal, confirming that $\text{Cu}_9\text{Fe}_9\text{S}_{16}$ is mechanically stable. As presented in Table 3, the elastic constants indicate that C_{33} is slightly larger than C_{11} , suggesting that the material exhibits marginally higher stiffness along the crystallographic c -axis compared to the a - and b -directions. Furthermore, C_{33} is significantly greater than the shear components C_{44} , C_{55} and C_{66} , which indicates that the material is mechanically anisotropic. The relatively low values of the shear elastic constants suggest that shear deformation is energetically more favourable than compressive or tensile deformation along the principal crystallographic axes. The Debye temperature is a key parameter related to various physical properties of solids, such as specific heat, thermal conductivity, and melting point. Notably, quantum effects become negligible above this temperature. For moohoekite the calculated Debye temperature is 318.7 K which shows reasonable agreement with the experimental value [6] (given in parentheses in Table 2).

GPa	C_{11}	C_{12}	C_{13}	C_{33}	C_{44}	C_{66}
$\text{Cu}_9\text{Fe}_9\text{S}_{16}$	118.53	69.10	72.84	124.44	27.94	32.5
"Elastic moduli	Bulk(B)	Shear(G)	Young's (E)	B/G	ν	Θ_D (K)

87.83	27.47	74.62	3.20	0.35	318.6(292)
-------	-------	-------	------	------	------------

“Table 2. Calculated elastic constants, C_{ij} (GPa), bulk modulus B(GPa), shear modulus G(GPa) and Young’s modulus (E) values of $\text{Cu}_9\text{Fe}_9\text{S}_{16}$ at 0 GPa and 0 K, together with the experimental data.”

3.3. Electronic properties

The density of states (DOS) is a fundamental tool for analyzing the electronic structure of materials, as it describes the number of electronic states at each energy level that are available. In this study, the total and partial density of states (DOS) for $\text{Cu}_9\text{Fe}_9\text{S}_{16}$ were computed using the GGA+U approach, the findings are illustrated in Figure 3. The total DOS (TDOS) reveals an overall spin symmetry between the spin-up and spin-down DOS, featuring significant contributions from both the valence and conduction bands, though the valence band had more density of states. The visible dominance of spin-up and spin-down symmetry in the DOS, suggest that the material exhibits a predominantly antiferromagnetic consistent with experimental findings. Importantly, the application of the Hubbard U correction leads to the emergence of a narrow band gap of approximately 0.5 eV near the Fermi level, suggesting semiconducting behavior as reported in literature, hence addressing the well-known tendency of standard GGA, which tend to underestimate band gaps [17].

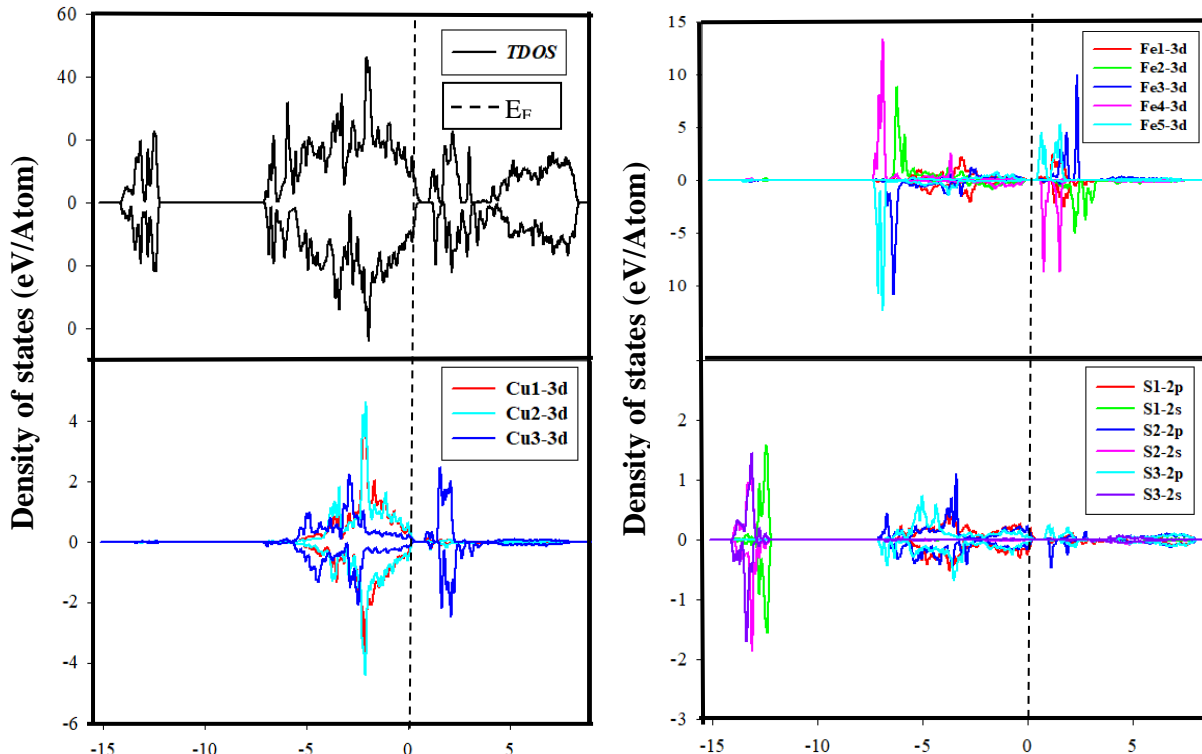


Figure 2. The total and partial density of states of $\text{Cu}_9\text{Fe}_9\text{S}_{16}$

The site-resolved PDOS of $\text{Cu}_9\text{Fe}_9\text{S}_{16}$ reveals a complex and highly diverse varied magnetic and electronic structure across its five distinct iron sites. In contrast, Fe2 and Fe3 exhibit display moderate spin polarization, characterized by sharp peaks just below the Fermi level, indicating finite magnetic moments and potential contribution to charge transport. Fe4 stands out due to pronounced spin asymmetry characterized by deep valleys and sharp peaks in its density of states, identifying it as a primary magnetic site with influence on low-energy electronic behaviour. Fe5, owing to its unique bonding environment, exhibits intense spin-polarized states at the Fermi level, indicative of strong magnetic behaviour. Meanwhile, the copper sites exhibit minimal magnetic activity, with Cu1 and Cu2 presenting fully occupied 3d states located deep in the valence band, characteristic of a Cu^{1+} oxidation state and contributing marginally to the magnetic and conduction properties. Cu3, however, displays a more active electronic profile near the Fermi level, suggesting a potential role in conduction and magnetic coupling. The sulfur atoms, characterized by deep 2s states and valence 2p states from approximately –

7 eV to 0 eV, form strong bonds with neighbouring Cu and Fe atoms. They remain nearly spin-symmetric, acting primarily as ligands that mediate magnetic interactions rather than carriers of magnetic moments.

4. Conclusion

In this study, first-principles density functional theory (DFT) calculations incorporating van der Waals dispersion corrections (DFT-D3) and Hubbard U correction were employed to systematically investigate the bulk properties of Mooihoeekite ($\text{Cu}_9\text{Fe}_9\text{S}_{16}$). The optimized structural parameters exhibit excellent agreement with experimental crystallographic data, thereby validating the reliability of computational approach. Electronic structure analysis reveals that Mooihoeekite is a narrow-gap semiconductor, with an estimated band gap of approximately 0.5 eV and displays antiferromagnetic ordering, as evidenced by the spin symmetry in both the total and projected density of states. A detailed site-resolved analysis highlights the varying magnetic behaviour of the five distinct Fe atoms, with Fe4 and Fe5 demonstrating strong spin polarization and contributing significantly to the overall magnetic character. In contrast, while the Cu atoms predominantly remain in a nonmagnetic Cu^{1+} state. The mechanical properties derived from the calculated elastic constants, confirm that the material is mechanically stable, anisotropic, and ductile, with a Pugh ratio (B/G) of 3.20 and a Poisson's ratio of 0.35. Furthermore, the calculated Debye temperature of 318 K aligns well-with experimental data, reinforcing the material's thermal stability under moderate conditions. Collectively, these results provide the first comprehensive computational insight into the structure–property relationships in Mooihoeekite. They serve as a valuable reference for future investigations of the surface chemistry, thermoelectric properties, and potential applications of Mooihoeekite in functional devices where semiconducting and magnetically active sulfide materials are of interest.

Acknowledgements

This research was conducted at the Materials Modelling Centre (MMC), University of Limpopo. We acknowledge the computational resources provided by the Centre for High Performance Computing (CHPC) and the financial support from the National Research Foundation (NRF).

4. References

- [1] F. Hulliger, Berlin, 1968, pp. 83-229.
- [2] M. Schlesinger, K. King, C. Sole and W. Davenport, *Extractive metallurgy of Copper*, pp. 13-30, 2011.
- [3] L. Cabri and S. Hall, *American mineralogist*, vol. 57, pp. 689-708, 1972.
- [4] S. Hall, *American mineralogist*, pp. 168-172, 1975.
- [5] D. Vaughan, K. England, G. Kelsall and Q. Yin, *American Mineralogist*, vol. 80, p. 725–731, 1995.
- [6] Q. Xianxiu, Q. Pengfei, D. Tingting, H. Hui, D. Xiaolong, S. Xun and C. Lidong, *Zeitschrift für anorganische und allgemeine Chemie*, vol. 646, pp. 1116-1121, 2020.
- [7] M. Townsend, J. Horwood, R. Hall and L. Cabri, *American mineralogist*, p. 10, 1972.
- [8] G. Kresse and J. Furthmuller, *Comput.Mater.Sci*, 1996.
- [9] G. Kresse and G. Joubert, *Phys. Rev. B: Condens. Matter*, 1999.
- [10] P. Blochl, *Phys. Rev B:Condensed Matter Phys*, p. 17953, 1994.
- [11] P. Perdew, K. Burke and M. Ernzerhof, *Phys. Rev. Lett.*, p. 1396, 1997.
- [12] B. Hımmetoglu, A. Floris, S. de Gironcoli and M. Cococcioni, *Int. J. Quantum Chem.*, p. 114, 2014.
- [13] S. Grimme, J. Antony, S. Ehrlich and J. Kriel, *J.Chem. Phys.*, p. 132, 2010.
- [14] H. Monkhorst and J. Pack, *Phys. Rev. B: Solid State*, p. 5188, 1976.
- [15] W. Zou, C. Tang and W. Lee, *International Journal of Solids and Structures*, pp. 2457-2467, 2013.
- [16] Z. Wu, E. Zhao, H. Xiang, X. Hao, X. Liu and J. Meng, *Phy.Rev B*, p. 054115, 2007.
- [17] Y. Li, Y. Liu, J. Chen, C. Zhao and C. Weiyong, *Physicochemical problems of mineral processing*, pp. 100-111, 2021.

